

UNCLASSIFIED

AD 282 735

*Reproduced
by the*

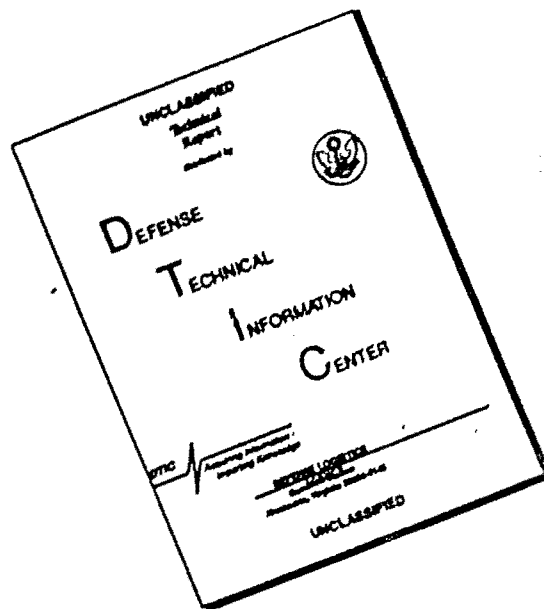
ARMED SERVICES TECHNICAL INFORMATION AGENCY
ARLINGTON HALL STATION
ARLINGTON 12, VIRGINIA



UNCLASSIFIED

NOTICE: When government or other drawings, specifications or other data are used for any purpose other than in connection with a definitely related government procurement operation, the U. S. Government thereby incurs no responsibility, nor any obligation whatsoever; and the fact that the Government may have formulated, furnished, or in any way supplied the said drawings, specifications, or other data is not to be regarded by implication or otherwise as in any manner licensing the holder or any other person or corporation, or conveying any rights or permission to manufacture, use or sell any patented invention that may in any way be related thereto.

DISCLAIMER NOTICE



THIS DOCUMENT IS BEST QUALITY AVAILABLE. THE COPY FURNISHED TO DTIC CONTAINED A SIGNIFICANT NUMBER OF PAGES WHICH DO NOT REPRODUCE LEGIBLY.

AEROSPACE CORPORATION

DISTRIBUTION

DATE 10 October 1962

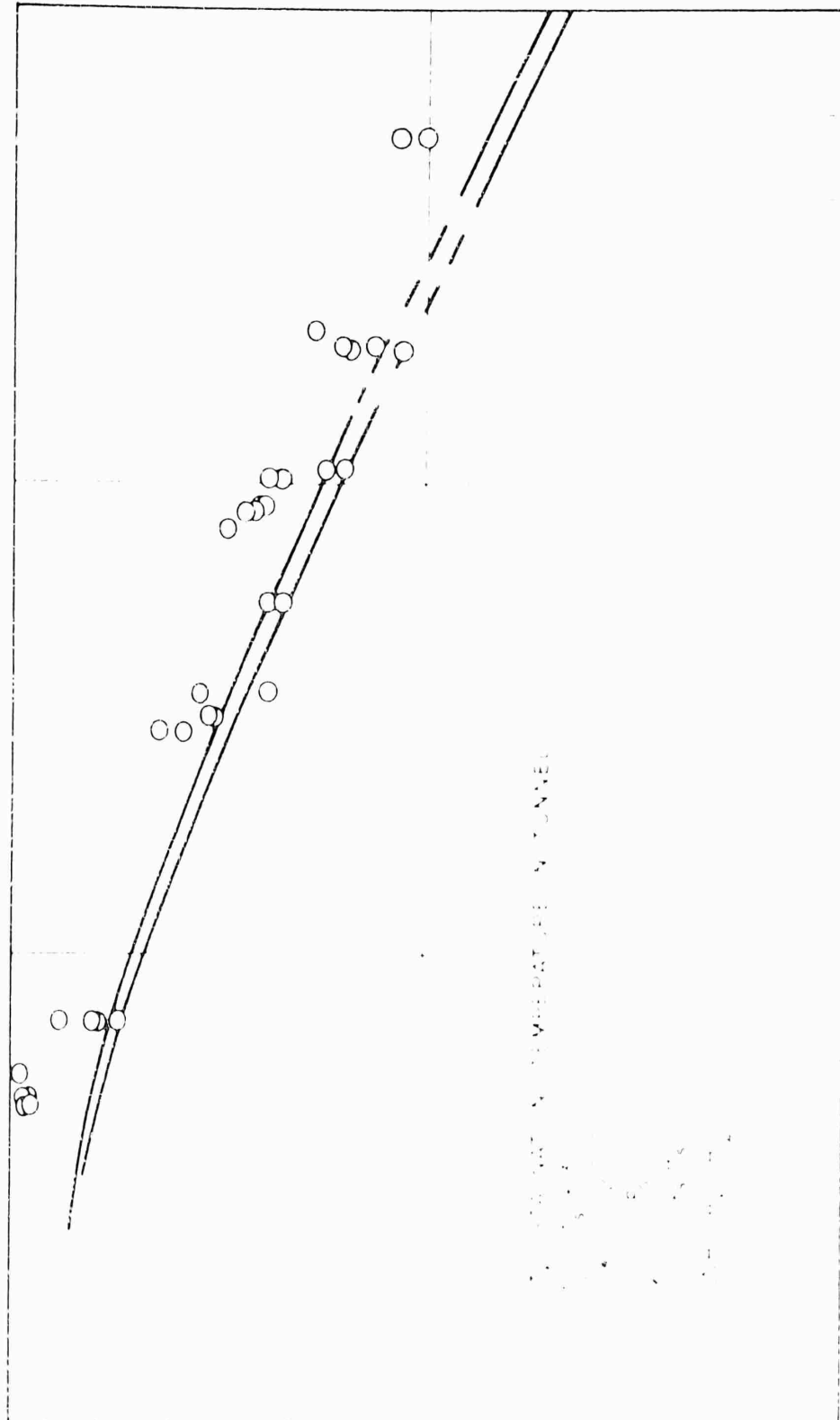
Subject: Errata, TDR-930(2230-11)TN-2

Prepared by: Robert L. Varwig

AD 282735

282 735

The attached corrected pages replace pages 4 and 14 of the report, "Stagnation Point Heat Transfer Measurements in Hypersonic Low Reynolds Number Flows," prepared by Robert L. Varwig, dated 5 June 1962. (Aerospace Corporation Report No. TDR-930(2230-11)TN-2.)



10²

$$h_c = 0.023 \frac{k}{D} \text{Re}^{0.8} \text{Pr}^{0.4}$$

FIG. 1. Comparison of Experimental Heat Transfer Rates With the Predictions of Ref. 2 for Cylinders

282 735

282 735

Stagnation Point Heat Transfer Measurements
in Hypersonic Low Reynolds Number Flows

5 JUNE 1962

Prepared by
ROBERT L. VARWIG
Aerodynamics and Propulsion Research Laboratory

Prepared for DEPUTY COMMANDER AEROSPACE SYSTEMS
AIR FORCE SYSTEMS COMMAND
UNITED STATES AIR FORCE
Inglewood, California

ASTIA
AUG 27 1962
TISIA

LABORATORIES DIVISION •

AEROSPACE CORPORATION

CONTRACT NO. AF 04(647)-930

DCAS-TDR-62-125

Report No.
TDR-930(2230-11)TN-2

STAGNATION POINT HEAT TRANSFER MEASUREMENTS
IN HYPERSONIC LOW REYNOLDS NUMBER FLOWS

Prepared by
Robert L. Varwig
Aerodynamics and Propulsion Research Laboratory

5 June 1962

AEROSPACE CORPORATION
El Segundo, California

Contract No. AF 04(647)-930

Prepared for
DEPUTY COMMANDER AEROSPACE SYSTEMS
AIR FORCE SYSTEMS COMMAND
UNITED STATES AIR FORCE
Inglewood, California

STAGNATION POINT HEAT TRANSFER MEASUREMENTS
IN HYPERSONIC LOW REYNOLDS NUMBER FLOWS

Prepared by Robert L. Varwig
Robert L. Varwig
Experimental Aerodynamics Department

Approved by J. G. Logan
J. G. Logan, Director
Aerodynamics and Propulsion
Research Laboratory

AEROSPACE CORPORATION
El Segundo, California

ABSTRACT

Measurements have been made of heat transfer rates at the stagnation point of cylinders and spheres for hypersonic flow at Reynolds numbers from 5 to 500 based on nose radius. A comparison of the measurements with the predictions of Probstein and Kemp, Ferri, Zakkay and Ting, and H. K. Cheng is considered. It is concluded that, within the experimental error, ordinary boundary layer theory can be used to predict the heat transfer rates down to stagnation point Reynolds numbers of twenty. At this point, the heat transfer rate increases somewhat as predicted, reaching the free molecule value at a Reynolds number between two and three.

CONTENTS

I.	INTRODUCTION.	1
II.	THEORETICAL PREDICTIONS.	3
III.	EXPERIMENTS	7
IV.	RESULTS	10
V.	CONCLUSIONS.	16
	NOMENCLATURE	17
	Table 1. Shock Tunnel Conditions and Experimental Heat Transfer Measurements	12
	REFERENCES.	18

FIGURES

1	View of Shock Tunnel Showing 12-in. Diameter Test Section in Place	2
2	Heat Transfer Rates to Cylinders as a Function of the Stagnation Point Reynolds Number According to Refs. 1 and 4	5
3	Heat Transfer Rates to Spheres as a Function of the Stagnation Point Reynolds Number According to Refs. 1, 3, and 4	6
4	20-mm Cylindrical Model Used in the Tests	8
5	Mounting Arrangement in the Tunnel for the Spherical Model Showing Pitot Tube.	8
6	Comparison of Experimental Heat Transfer Rates With The Predictions of Ref. 2 for Cylinders.	14
7	Typical Temperature History for the Stagnation Point of Cylindrical Model.	16

I. INTRODUCTION

Considerable interest has been generated in the determination of the heat transfer rates to hypersonic vehicles in the Reynolds number range between the free molecule flow regime and the continuum regime. This range corresponds to the flow conditions in which hypersonic glide vehicles with their shallow re-entry paths may find themselves for an extended time. Strictly speaking, one should not expect to apply continuum boundary layer flow theory to this regime in the conventional manner. Theoretical analyses have been developed^{1, 2, 3} for this rarefied gas regime but are, for the most part, unsubstantiated by experiment. It is, therefore, the purpose of this study to attempt to measure the stagnationpoint heat transfer rates to cylinders and spheres in the hypersonic shock tunnel at flow Mach numbers from 13 to 23. The Reynolds number range to be covered is from 5 to 500 (based on nose radius) corresponding to the regime between free molecule flow and the continuum range.

Because of its high reservoir stagnation temperature, the shock tunnel is an instrument uniquely suited to making measurements at high Mach numbers and low Reynolds numbers typical of the high altitude portions of the launch trajectory of satellite vehicles. Furthermore, the shock tunnel can yield a variety of pressures, and, hence, Reynolds numbers for a given stagnation temperature. The chief drawback, inherent in shock tunnels, is the comparatively short time interval during which measurements can be made. As a result, equilibrium conditions between the flow and the measuring instrument usually cannot be obtained and must be inferred from the transient response of the measuring device. In this report, heat transfer rate measurements determined from the transient response of thin film resistance thermometers mounted at the stagnation point of models are described, and the results of the measurements presented. The shock tunnel facility in which these tests were made is shown in Fig. 1.

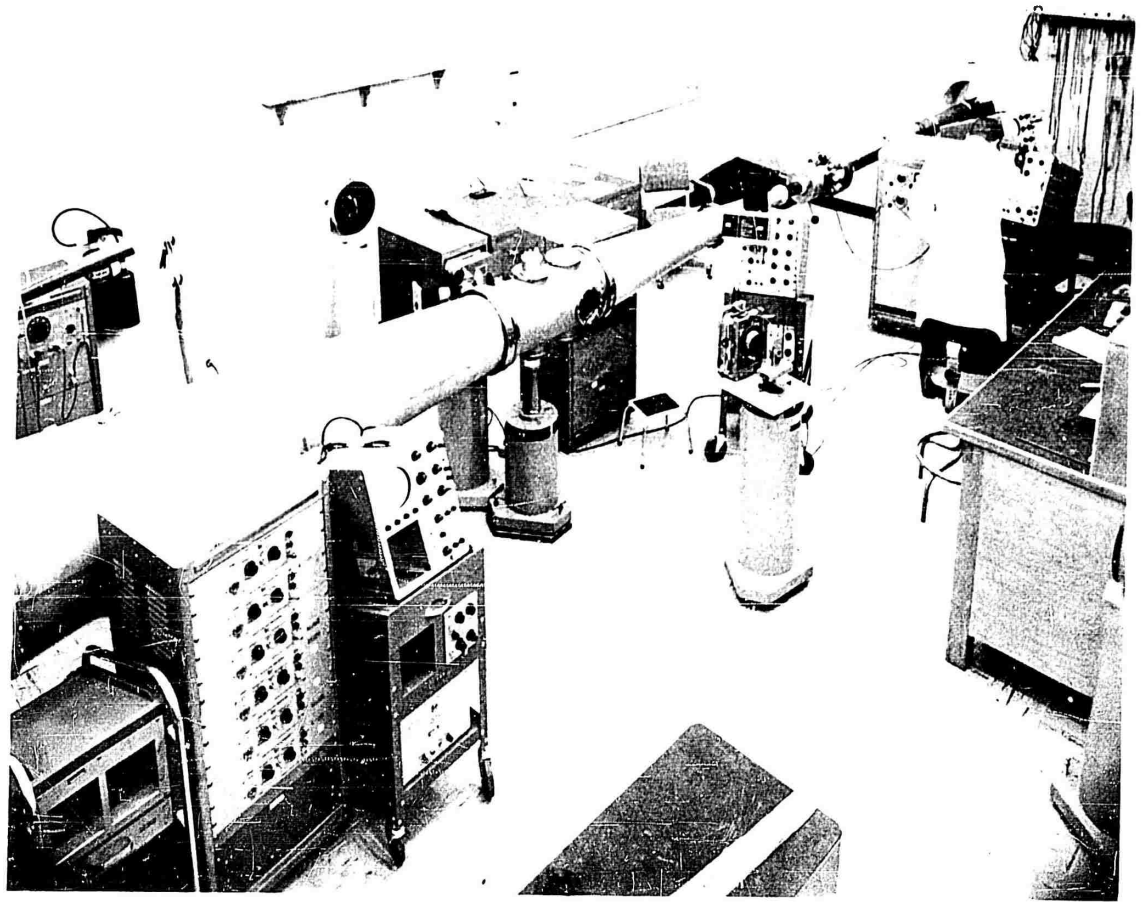


Fig. 1. View of Shock Tunnel Showing 12-in. Diameter Test Section in Place

II. THEORETICAL PREDICTIONS

Probstein and Kemp¹ have considered the problem of calculating the aerodynamic heating to be expected in hypersonic rarefied gas flows where the mean free path becomes too large for the use of the inviscid flow-boundary layer approach and too small for the free molecule flow regime to apply. They have solved the Navier-Stokes equations for two sets of boundary conditions: (1) a "viscous layer" class in which a thin shock wave exists, but in which the region between the shock and the blunt body is fully viscous; and (2) a "merged layer" class representing a more rarefied condition. In the merged layer, the shock wave is no longer thin, and the Navier-Stokes equations are used to provide a solution which includes the shock structure and has free stream conditions as outer boundary conditions.

Probstein and Kemp have carried out numerical calculations for a sphere and a cylinder, assuming constant density in the shock layer, and have predicted from these calculations a different stagnation point heat transfer rate from that to be expected on the basis of extrapolated boundary layer theory. The viscous layer theory predicts higher heat transfer to both spheres and cylinders normal to the flow as the Reynolds number (based on nose radius) is decreased to the order of 10. The incipient merged layer theory modifies the heat transfer rates to values which are less than in the viscous layer, but are still greater than in the boundary layer theory.

In Cheng's² analysis, the flow field around the body is divided into two regions: the shock-transition zone and the shock layer, both of which are regions assumed to be thin compared to the characteristic dimensions of a body. Across the shock transition zone, the Rankine-Hugoniot relations, modified to include tangential stress and heat conduction terms, are assumed to hold, but the shock is still treated as thin. In the shock layer region, the Navier-Stokes equations govern the flow which is assumed to be a continuum. No constant density assumption is made regarding the flow in the shock layer, and the solution, although approximate, represents a less restrictive approach.

Cheng also considers two regimes roughly analogous to the viscous layer and incipient merged layer of Probstein and Kemp. In the regime where the viscosity and heat conduction effects cannot be ignored in the shock transition zone, Cheng predicts a substantial reduction in the temperature behind the shock wave. He predicts heat transfer rates in the viscous layer regime essentially equivalent to those predicted by the analysis of Probstein and Kemp. No attempt was made to compare the theoretical results of the two analyses for the regime which corresponds to the incipient merged layer.

In the approach taken by Ferri, Zakkay, and Ting³ at Brooklyn Polytechnic Institute, the boundary layer concept is retained and modified. They show that for bodies of practical size, the effects of viscosity and conductivity in the flow outside the boundary layer modify the heat transfer rate at the wall in the region between the stagnation point and the sonic point by less than 5% for Reynolds numbers as low as 30 (based on nose radius). The Brooklyn group indicates that, at low Reynolds numbers, the shear produced in the boundary layer by the shock-induced vorticity becomes of the same order as the shear stress at the wall. Hence, they include the effect of the vorticity in the boundary layer analysis.

The heat transfer rate predictions based on these theories are compared with those of boundary layer theory and free molecule flow in Fig. 2 and 6 (for cylinders) and Fig. 3 (for spheres). Heat transfer rates based on boundary layer theory are calculated according to the work of Fay and Riddell.⁴ The free molecule flow value, plotted according to the parameters specified by Cheng, is represented by a value of $\dot{q}/\rho U \Delta H$ equal to 1. The predictions of Probstein and Kemp are given for cylinders and for spheres in the viscous layer, and for spheres in the merged layer. Although an incipient merged layer prediction for the cylinder is not made, it is easy to suppose that it lies between the value of the viscous layer theory and the boundary layer theory. These curves were computed on the basis of a density ratio of 0.1 across the shock and a γ of 11/9 for the gas.

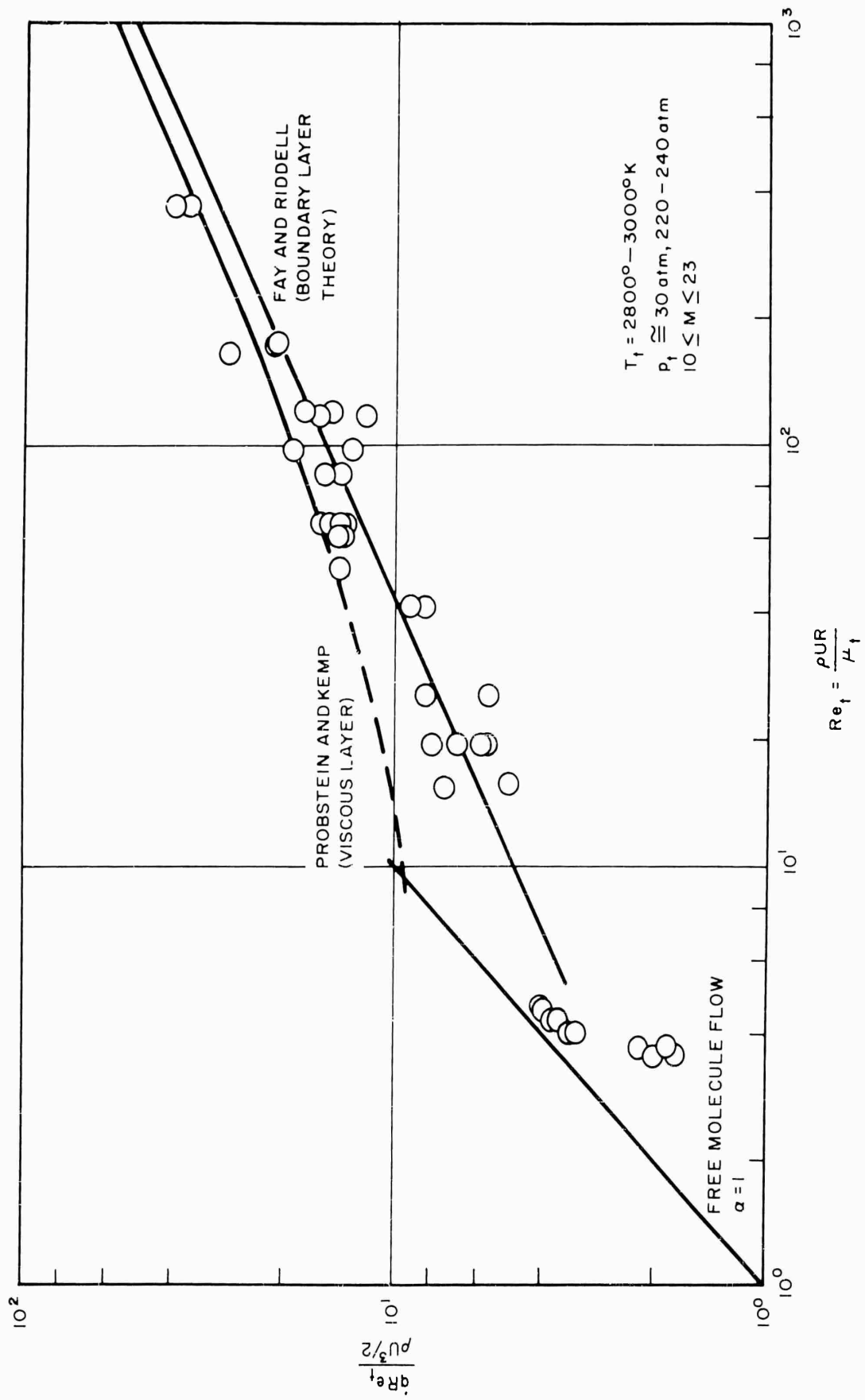


Fig. 2. Heat Transfer Rates to Cylinders as a Function of Stagnation Point Reynolds Number According to Refs. 1 and 4

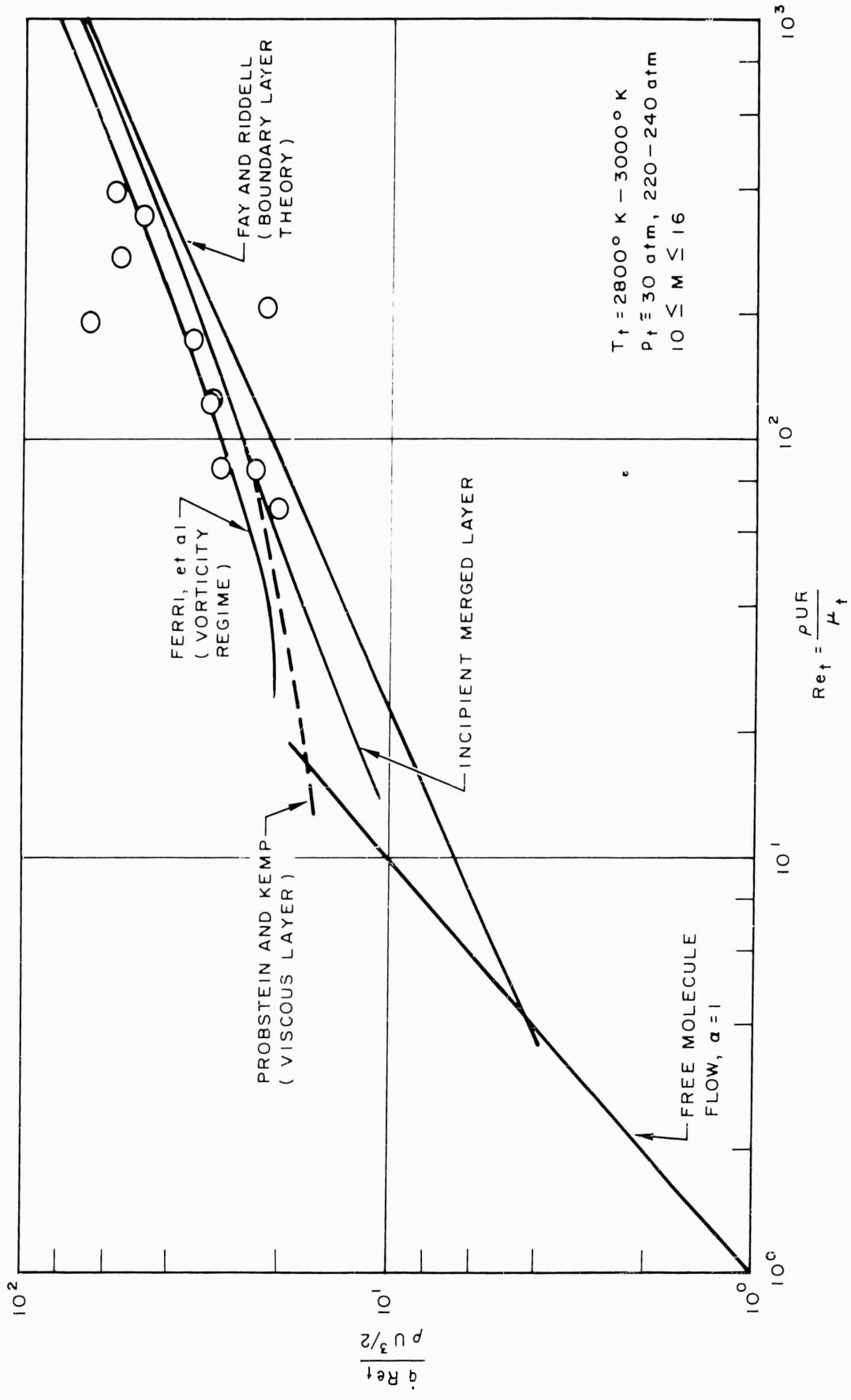


Fig. 3. Heat Transfer Rates to Spheres as a Function of Stagnation Point Reynolds Number According to Refs. 1, 3, and 4

III. EXPERIMENTS

In the shock tunnel for shock Mach numbers of 4.5 to 4.7, reservoir test conditions between 220 and 240 atm and 2840 and 3000°K are obtained. These conditions remain steady for about 4 ms. Using the 12-in. diameter test section and varying the throat diameter over a range from 0.04 to 0.375 in. yields Mach numbers from 10 to 23. For each test, the shock Mach number in the shock tube, M_s , and the pitot pressure in the test section, p_t' , are determined. The conditions behind the reflected shock, that is, the reservoir conditions, are ascertained from the shock Mach number. These conditions along with the pitot pressure measurement determine the flow Mach number in the test section.

Spherical and cylindrical shells of pyrex brand 7740 glass, ranging in diameter from 3 to 20 mm, were employed as models. Two thin film resistance thermometers were applied on the cylindrical models at the stagnation point and half an inch on either side of the midpoint of the cylinder. The films were applied by airbrushing Hanovia No. 05X liquid bright platinum paint in a strip 0.5 mm wide and half an inch long, and then firing at 1250°F. Firing the silver micro paint in a heavy layer provided low resistance contacts with the measuring circuit. Figure 4 is a photograph of the cylindrical model. This model was mounted in the test section normal to the flow such that the midpoint of the cylinder corresponded to the axis of the tunnel test section. The cylinder was cantilevered from the wall. The spherical model has a shorter thin film at its stagnation point and is supported from the model stand as shown in Fig. 5. The pitot pressure gauge location is indicated in this photograph.

The technique of thin film resistance thermometry is quite well known and very adequately covered in the literature. In essence, the thermometer measures the surface temperature history of the material upon which it resides. This recorded temperature history is converted to a heat transfer rate by one-dimensional heat conduction theory and one basic calibration of the thermometer. The basic calibration is generally done by the pulsing technique



Fig. 5. Mounting Arrangement in the Tunnel for the Spherical Model Showing Pitot Tube

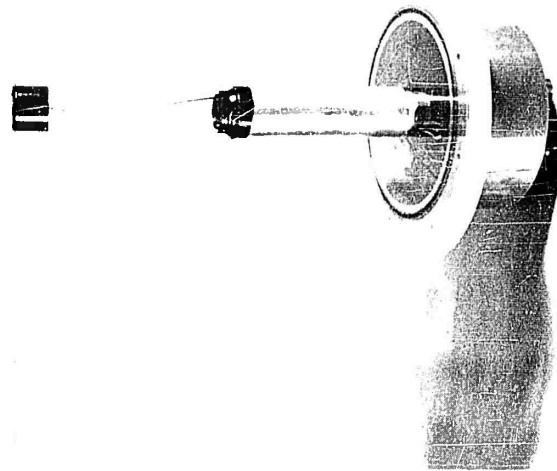


Fig. 4. 20-mm Diameter Cylindrical Model Used in Tests

Two thin film resistance thermometers are mounted parallel to the axis of the cylinder at the stagnation point

where a known heat flux, produced by a current step pulse through the resistance thermometer, is applied to the gauge. The calibration determines the lumped thermal properties of the substrate of the thin film, $\sqrt{\pi \rho C k}$, where ρ , C , and k are the density, specific heat, and conductivity of the substrate, respectively. The thermal coefficient of resistance of the film is determined by measuring its resistance at the freezing and boiling points of water.

The equation relating the heat transfer rate, \dot{q} , of the model with temperature history of the model surface, $(\Delta T/\sqrt{t})$, is

$$\dot{q} = \frac{\sqrt{\pi \rho C k}}{2} \left\{ 1 + \frac{b}{k_0} \left[\left(1 + \frac{\Delta T}{T_0} \right) \left(\frac{T_0}{\Delta T} \right) \log_{10} \left(1 + \frac{\Delta T}{T_0} \right) - 0.434 \right] \right\} \frac{\Delta T}{\sqrt{t}}$$

where ΔT is the temperature change of the surface, and T_0 is the initial temperature of the surface. The quantity in the brackets $\left\{ \right\}$ represents the correction to the heat transfer rate which must be added to account for the change in the thermal properties of the substrate when the surface temperature becomes large compared to the calibration temperature.⁵ In this equation, b/k_0 is a constant characteristic of the material being used, and, for pyrex, it is equal to 4.73.

In the shock tunnel, measurements were made of the heat transfer rates to cylinders with diameters of 3 mm, 10 mm, and 20 mm, and to spheres with diameters of 10 and 20 mm. Reservoir stagnation conditions ranged from 2800 to 3000°K, with pressures of 28 to 29 atm, and 220 to 240 atm. Mach numbers in the test section varied from 10 to 23 with most of the data in the range from 13 to 16.

IV. RESULTS

The results of the calculations of Probstein and Kemp are presented as $\dot{q}/(\rho U^3/2)$ as a function of the stagnation point Reynolds number $\rho U R_b/\mu_t$. Here, ρ and U are the free stream density and velocity, μ_t is the viscosity evaluated at the stagnation temperature of the gas behind the bow shock, and R_b is the radius of the sphere or cylinder.

Ferri, Zakkay, and Ting have presented heat transfer rate predictions in the form of the ratio of the heat transfer rate including vorticity to the rate for zero vorticity determined from Fay and Riddell's work. This ratio was plotted as a function of the Reynolds number defined as

$$Re = \frac{R_b \rho_t \sqrt{H_{se}}}{\mu_t}$$

where $H_{se}/H_t \approx 1$. Their value of the Reynolds number is about 6.4 times as large as the Re_t defined by Probstein and Kemp. Taking these differences into account, the predictions of Ferri, et al are presented with those of Probstein and Kemp.

Cheng has presented his results in the form of Stanton number, $C_H = \frac{\dot{q}}{\rho U \Delta H}$, as a function of k^2 ; ρ and U having the same meaning as above. Also, $\Delta H = H_t - H_w$, where H_t is the total gas enthalpy and H_w is the enthalpy evaluated at the body temperature (i. e., $\sim 300^\circ K$); k^2 is related to the stagnation point Reynolds number, Re_t , by the equation

$$k^2 = \epsilon Re_t \left(\frac{T_* \mu_t}{T_t \mu_*} \right)$$

where

$$\epsilon = \frac{P_s}{2\rho_s H_s}$$

$$T_* = \frac{T_s + T_w}{2}$$

and T'_t is the stagnation point temperature behind the normal shock. The subscript s refers to conditions behind the normal shock.

The experimental values of the reservoir conditions, the flow Mach numbers, and the heat transfer rates obtained in this study are listed in Table 1. Values of $(\dot{q} Re_t)/(1/2 \rho U^3)$ as a function of Re_t are plotted in Figs. 2 and 3, along with the theoretical results of Probstein and Kemp and the boundary layer predictions of Ferri, et al and Fay and Riddell. To calculate the values of Re_t , the values of viscosity were determined according to the results of studies recently reported by Hartunian and Marrone for oxygen.⁶ They indicate that the Sutherland viscosity values based on kinetic theory and hard spherical molecules are as much as 50% low for temperatures up to 3000°K. This modified value of μ_t was also used to determine the theoretical value of \dot{q} from Fay and Riddell.

The experimental results for the cylinder seem to agree with the boundary layer theory right down to the free molecule flow regime, with only a small increase in the heat transfer rate at Reynolds numbers less than 20.

In order to compare the experimental results with the predictions of Cheng, the strong cooling that was predicted had to be accounted for. This was accomplished by an iteration as follows: The value of ϵ was first determined, using the experimentally measured value of pitot pressure (the total pressure behind the shock) for p_s ; and ρ_s and H_s were estimated from real gas calculations, given the flow Mach number and the initial reservoir conditions. The value of T_s was estimated, and t_{**} , μ_{**} , and, finally, k^2 were computed. Using Fig. 3 of Cheng² and k^2 , a value for the entropy function, $(H_s - H_\omega)/(H_t - H_\omega)$, was selected from which H_s and T_s could be determined, then H_s was substituted back into the equation for ϵ and a new k^2 was determined using this ϵ and the new T_s . The values of k^2 and ϵ usually converged after three iterations. The experimental heat transfer rate, \dot{q} , in the form of Stanton number, is plotted as a function of k^2 .

Figure 6 is a comparison of the predicted and experimental results for cylinders for values of $0.4 < k^2 < 50$ corresponding to values of $5 < Re_t < 500$.

Table 1

Shock Tunnel Conditions and Experimental Heat Transfer Measurements

Cylinders							
M_s	P_t , atm	T_t , $^{\circ}K$	p_t' , atm	M	R, cm	Re_t	q , watts/cm ²
4.63	233	3047	0.125	13.0	0.15	61.9	386 390
4.63	222	2980	0.0445	16.0	0.15	25.6	143 208
4.79	243	3100	0.0410	16.5	0.15	19.4	160 158
4.75	235	3050	0.00818	23.7	0.15	4.01	82.6 86
4.75	240	3060	0.00855	23.5	0.15	4.3	91.8 94
4.73	239	3120	0.1125	13.5	0.15	51.1	393
4.71	228	3020	0.0434	16.2	0.15	19.4	179 207
4.68	229	3016	0.00945	22.8	0.15	4.51	100
4.75	239	3070	0.0408	16.5	0.495	64.9	121 128
4.66	224	3000	0.0424	16.4	0.495	64.7	108 99.4
4.70	226	3020	0.1107	13.4	1.03	370	149 137
4.70	234	3102	0.101	13.5	0.495	164	261
4.73	227	3040	0.0386	16.4	1.03	117	69.3 53.1
4.73	227	3090	0.0408	16.3	1.03	121	77.2 64.4
4.51	29	2870	0.0197	12.3	1.03	84.5	45.7 40.7
4.47	30	2860	0.0210	12.3	0.495	41.3	63.3 58.1
4.45	27.9	2847	0.0444	10.3	1.03	175	70.4 69.6
4.54	29.8	2946	0.0592	9.85	0.495	97.4	131 91.8

Table 1 (continued)

Spheres							
M_s	p_t , atm	T_t , $^{\circ}K$	p_t' , atm	M	R, cm	Re_t	\dot{q} , watts/cm ²
4.67	226	3000	0.1147	13.22	0.520	190	556
4.67	234	3030	0.1147	13.35	0.493	174	313
4.65	220	2980	0.0434	15.95	0.536	83.4	144
4.64	226	3000	0.0402	16.3	0.501	68.9	149
4.73	236	3060	0.0390	16.5	0.996	126	124
4.77	237	3070	0.0369	16.7	1.00	125	122
4.74	224	3050	0.1045	13.5	1.04	391	203
4.68	220	2970	0.0966	13.6	1.05	341	172
4.46	27.9	2843	0.0576	9.65	1.03	207.6	71.3
4.38	30.1	2784	0.0543	10.1	1.00	86.5	244

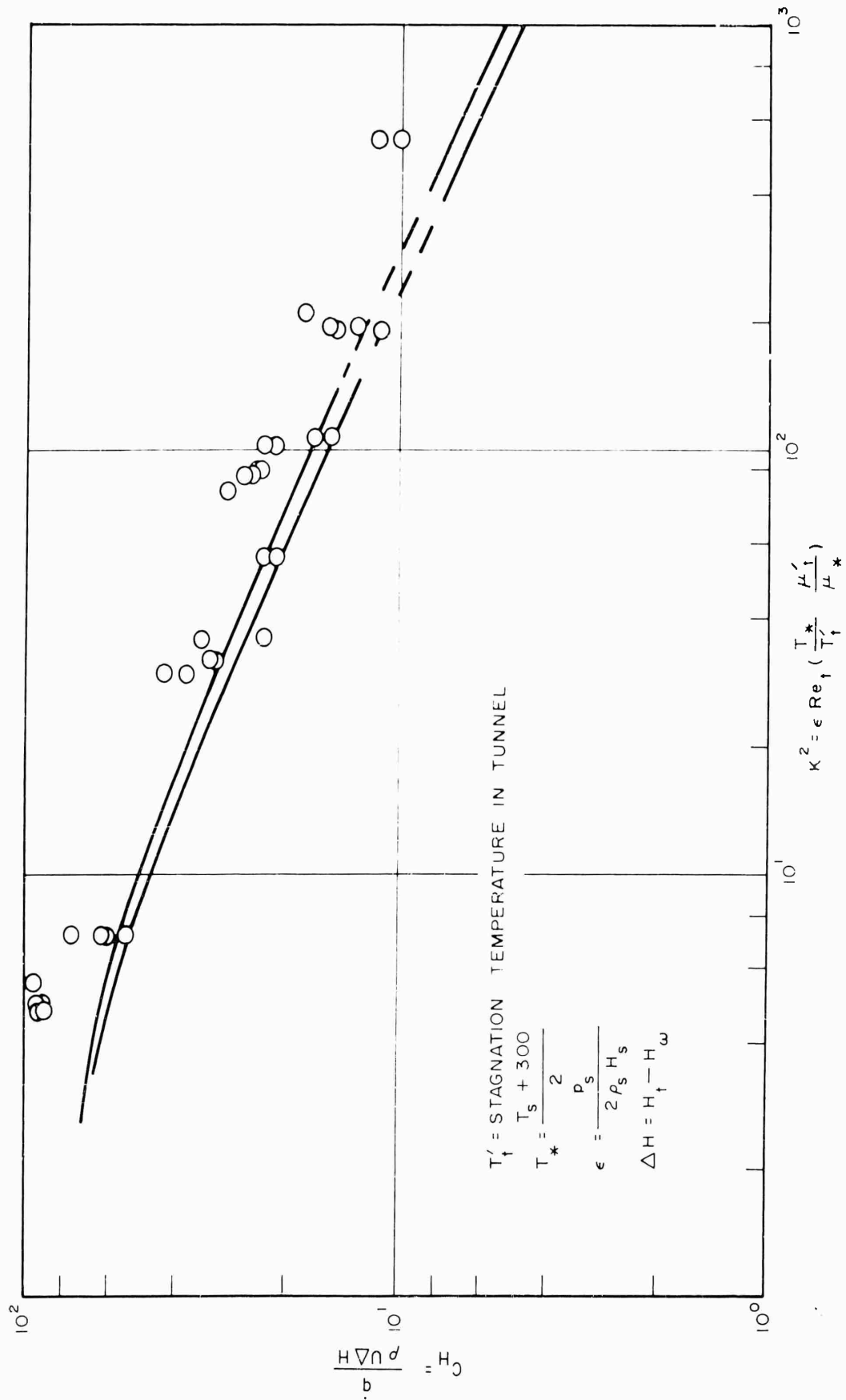


Fig. 6. Comparison of Experimental Heat Transfer Rates With the Predictions of Ref. 2 for Cylinders

As seen in Fig. 6, the experimental results again seem to assume a straight line, indicating, on the average, slightly higher heat transfer rates than those predicted. The portion of the curve in Cheng's theory corresponding to high values of Re_t is based on the continuum boundary layer theory of Cohen and Reshotko.⁷ Their theory predicts values for the heat transfer rate slightly lower than those of Fay and Riddell which seem to agree fairly well with the experimental data.

The considerable scatter in the data for both cylinders (Figs. 2 and 6), and spheres (Fig. 3) makes a definitive determination of the best theory impossible. The best that can be said is that the boundary layer theory can probably be used to predict heat transfer rates down to the free molecule flow regime within our ability to measure it. The corrections offered by Refs. 1, 2, and 3 are small; in general, less than the scatter in the data.

Since scatter in the data is present, some remarks on the accuracy of these experiments should be made. The shock Mach number can be measured to $\pm 1\%$, and, consequently, this is about the error expected in the reservoir conditions. The total pressure can be measured to within $\pm 10\%$, and this should be the expected error in ρ . As a result, the theoretical curve which is plotted from the experimentally obtained tunnel conditions can be considered to have a width of $\pm 10\%$. The heat transfer measurements have an uncertainty of between $\pm 5\%$ and $\pm 18\%$, depending upon how smooth and unambiguous the heat transfer record is. An example of an adequate record is shown in Fig. 7 for a flow Mach number of 16.0 and reservoir conditions of 222 atm and 2980°K.

No explanation is immediately available for the fact that there is greater scatter in the sphere data. Since the spheres were blown from pyrex tubing, some irregularities existed in their radii. However, the heat transfer rate depends inversely on the square root of the body radius and, hence, irregularities in the radius should not produce significant effects. The much smaller gauge on the spheres may limit the accuracy of the results.

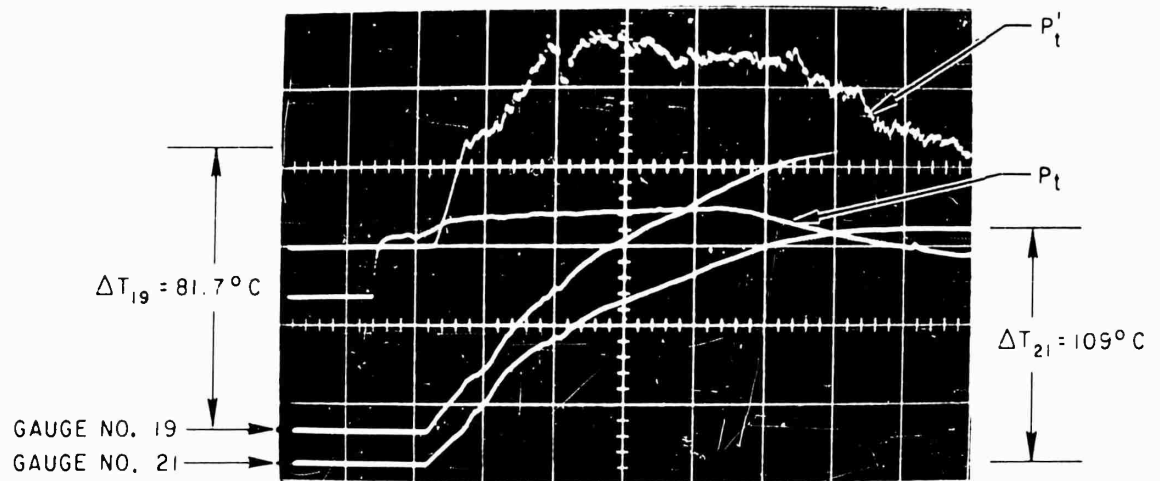


Fig. 7. Typical Temperature History for the Stagnation Point of a Cylindrical Model

$$P_t = 222 \text{ atm} \quad T_t = 2980^\circ\text{K} \quad M = 16.0$$

V. CONCLUSIONS

The heat transfer rate to cylinders and spheres, as measured in the shock tunnel, is adequately predicted by the theory of Fay and Riddell down to stagnation point Reynolds numbers of 20. At this point, the heat transfer rate increases somewhat over that predicted by Probstein and Kemp, reaching the free molecule flow heat transfer rate at a value of Re_t between 2 and 3.

NOMENCLATURE

H_s	Enthalpy behind the shock wave
H_{se}	Reference stagnation enthalpy (Ref. 3)
H_t	Total enthalpy
H_w	Enthalpy at the model wall temperature
M	Test section flow Mach number
M_s	Shock Mach number in the shock tube
p_s	Pressure behind the shock wave
p_t	Reservoir total pressure
p'_t	Test section pitot pressure
\dot{q}	Stagnation point heat transfer rate
R_b	Cylinder or sphere radius
T_s	Temperature behind the shock wave
T_t	Reservoir total temperature
T'_t	Model stagnation temperature
T_w	Model wall temperature
T_*	Reference temperature (Ref. 2) = $(T_s + T_w)/2$
U	Free stream velocity
ϵ	$p_s/2\rho_s H_s$
μ_t	Viscosity at model stagnation temperature
μ_*	Viscosity at reference temperature (Ref. 2)
ρ	Free stream density
ρ_s	Density behind the shock wave

REFERENCES

1. Probstein, R. F., Kemp, N. H., Viscous Aerodynamic Characteristics in Hypersonic Rarefield Gas Flow, Journal of the Aero/Space Sciences Vol. 27, No. 3, pp. 174-192, March 1960.
2. Cheng, H. K., Hypersonic Shock-Layer Theory of the Stagnation Region at Low Reynolds Number, Proc. of 1961 Heat Transfer and Fluid Mechanics Institute, held at Univ. of Southern Calif., June 1961.
3. Ferri, A., Zakkay, V., Ting, L., Blunt-Body Heat Transfer at Hypersonic Speed and Low Reynolds Numbers, Journal of the Aero/Space Sciences, Vol. 28, No. 12, pp. 962-971, December 1961.
4. Fay, J. A., Riddell, F. R., Theory of Stagnation Point Heat Transfer in Dissociated Air, Journal of the Aeronautical Sciences, Vol. 25, No. 2, pp. 73-85, February, 1958.
5. Hartunian, R. A., Varwig, R. L., On Thin-Film Heat Transfer Measurements in Shock Tubes and Shock Tunnels, Phys. Fluids, Vol. 5, No. 2, pp. 169-174, February 1962.
6. Hartunian, R. A., Marrone, P. V., Viscosity of Dissociated Gases from Shock-Tube Heat-Transfer Measurements, Phys. Fluids, Vol. 4, No. 5, pp. 535-543, May 1961.
7. Reshotko, E., Cohen, C. B., Heat Transfer at the Forward Stagnation Point of Blunt Bodies, NACA TN 3513, July 1955.

The five included volume of Reynolds number has
been two and three

UNCLASSIFIED

The five included volume of Reynolds number has
been two and three

UNCLASSIFIED

The five included volume of Reynolds number has
been two and three

UNCLASSIFIED

The five included volume of Reynolds number has
been two and three

UNCLASSIFIED

UNCLASSIFIED	<p>the free molecule value at Reynolds number between two and three</p>
--------------	---

UNCLASSIFIED	<p>the free molecule value at Reynolds number between two and three</p>
--------------	---

UNCLASSIFIED	<p>the free molecule value at Reynolds number between two and three</p>
--------------	---

UNCLASSIFIED	<p>the free molecule value at Reynolds number between two and three</p>
--------------	---